

Magnetic excitation and superconductivity in overdoped $\text{TiSr}_2\text{CaCu}_2\text{O}_{7-\delta}$: A ^{63}Cu NMR study

K. Magishi, Y. Kitaoka, G.-q. Zheng, and K. Asayama

Department of Material Physics, Faculty of Engineering Science, Osaka University, Toyonaka, Osaka 560, Japan

T. Kondo, Y. Shimakawa, T. Manako, and Y. Kubo

Fundamental Research Laboratories, NEC Corporation, 34 Miyukigaoka, Tsukuba 305, Japan

(Received 15 May 1996)

We report extensive measurements of the Knight shift K , the nuclear spin-lattice relaxation rate $1/T_1$, and the Gaussian spin-echo decay rate $1/T_{2G}$ of ^{63}Cu in overdoped $\text{TiSr}_2\text{CaCu}_2\text{O}_{7-\delta}$ (Ti1212) with $T_c = 70$ K, 52 K, and 10 K, in order to elucidate the origin of the reduction in T_c with increasing holes and to identify the symmetry of the order parameter. In the normal state, it is shown that $1/T_1T$ obeys the Curie-Weiss law, pointing to the presence of the antiferromagnetic (AF) spin correlation. From the analyses of $1/T_1$ and $1/T_{2G}$, it is found that the increase of the hole content in Ti1212 compounds makes the characteristic energy of the AF spin fluctuation around a zone boundary, $Q = (\pi/a, \pi/a)$, Γ_Q , transfer to a higher-energy region and concomitantly reduces the magnetic correlation length ξ_m significantly. The AF spin correlation is concluded to become less distinct in going from the optimum-doped to the overdoped regime. In the superconducting state, the T dependences of K and $1/T_1$ have revealed that the superconductivity is in the gapless regime with a finite density of states at the Fermi level. The NMR results are consistently interpreted in the d -wave model in which the impurity scattering is incorporated in terms of the unitarity limit as demonstrated in most of the high- T_c cuprates so far. Eventually, the reduction in T_c from 70 K to 52 K in Ti1212 is concluded to be not due to the impurity effect associated with the oxygen content. In the previous works, the enhancement of T_c from 93 K in $\text{YBa}_2\text{Cu}_3\text{O}_7$ with double CuO_2 layers to 115–135 K in $\text{Ti}_2\text{Ba}_2\text{Ca}_2\text{Cu}_3\text{O}_{10}$ and $\text{HgBa}_2\text{Ca}_2\text{Cu}_3\text{O}_{8+\delta}$ with triple CuO_2 layers was shown to be due to the increase in Γ_Q with ξ_m unchanged appreciably. This finding was compatible with the relationship of $T_c \propto \Gamma_Q \xi_m^2 \exp(-1/\lambda)$ based on the spin-fluctuation-induced mechanism for the d -wave superconductivity. Within the same scheme, the origin of the marked decrease in T_c irrespective of increasing Γ_Q in Ti1212 is proposed to be due to the significant reduction in ξ_m which makes the pairing interaction weaken and λ in the above formula reduced. [S0163-1829(96)03838-6]

I. INTRODUCTION

In order to explore the mechanism of high- T_c superconductivity, numerous works have been carried out on various high- T_c cuprates, e.g., underdoped $\text{La}_{2-x}\text{Sr}_x\text{CuO}_4$ (LSCO), overdoped $\text{Ti}_2\text{Ba}_2\text{CuO}_{6+\delta}$ (Ti2201) with a single CuO_2 layer, $\text{YBa}_2\text{Cu}_3\text{O}_{6+x}$ (YBCO $_{6+x}$), $\text{YBa}_2\text{Cu}_4\text{O}_8$ (Y124), $\text{YBa}_2\text{Cu}_3\text{O}_7$ (YBCO $_7$), $\text{Bi}_2\text{Sr}_2\text{CaCu}_2\text{O}_8$ (Bi2212) with double CuO_2 layers, and $\text{Ti}_2\text{Ba}_2\text{Ca}_2\text{Cu}_3\text{O}_{10}$ (Ti2223) and $\text{HgBa}_2\text{Ca}_2\text{Cu}_3\text{O}_{8+\delta}$ (Hg1223) with triple CuO_2 layers.¹ It is well known that the normal state properties of high- T_c cuprates are unusual, such as the T -linear resistivity and the anomalous T dependence of the Hall coefficient, etc.¹ In particular, the magnetic properties in underdoped compounds are quite unusual. Namely, the spin susceptibility $\chi_s(T)$ decreases upon cooling. The nuclear spin-lattice relaxation rate of ^{63}Cu , $^{63}(1/T_1)$, does not obey a $T_1T = \text{const}$ relation, but $^{63}(1/T_1T)$ follows a Curie-Weiss law above T_c in LSCO and YBCO $_7$,² whereas it exhibits a peak far above T_c in YBCO $_{6+x}$ (Refs. 3,4) and Y124.⁵ The latter result was argued to provide an evidence for a spin gap behavior; that is, a low-energy part of the spin fluctuation is suppressed before the onset of the superconductivity as also shown by neutron inelastic scattering experiments.⁶ The spin gap behavior has drawn much attention with the expectation that superconductivity may occur in a new framework of the spin-charge separation based on a resonating valence bond (RVB)

model.⁷ However, whereas the spin gap behavior was reproduced in the bilayer compound $\text{TiSr}_2(\text{Lu}_{1-x}\text{Ca}_x)\text{Cu}_2\text{O}_y$ even though a disorder was introduced into the Ca layers by substituting Lu to control holes and the CuO chains are absent,⁸ it was not observed for LSCO with a single CuO_2 plane even in the vicinity of the superconducting to magnetic phase boundary.⁹ Therefore, it is still controversial whether or not spin gap behavior is relevant to a superconducting mechanism.

In contrast, in the optimum-doped YBCO $_7$ and overdoped Ti2201 compounds where T_c decreases with increasing holes,¹⁰ $\chi_s(T)$ deduced from the Knight shift of ^{63}Cu is T independent, whereas $^{63}(1/T_1T)$ increases down to T_c ,¹¹ as well as in LSCO,² although its magnitude is considerably reduced with increasing holes. The Curie-Weiss T dependence of $^{63}(1/T_1T)$, which is rather commonly seen in most of high- T_c materials than the spin gap behavior, has been described in terms of the self-consistent-renormalization (SCR) theory,¹² the phenomenological antiferromagnetic (AF) spin fluctuation model,¹³ and by various approaches.^{7,14,15} A further remarkable finding was that the overdoped Ti2201 compounds, in which the AF spin fluctuation was not appreciable, no longer exhibited superconductivity, instead showing the $T_1T = \text{const}$ relation in a wide T range.¹¹ These results have suggested that the AF spin correlation plays a role for the occurrence of the superconductivity.

As a matter of fact, from extensive NMR measurements

involving the Knight shift K , the nuclear spin-lattice relaxation rate $1/T_1$, and the Gaussian spin-echo decay rate $1/T_{2G}$ of ^{63}Cu in the normal state of Tl2223 (Ref. 16) and Hg1223 (Ref. 17) with triple CuO_2 layers, we have found that the characteristic energy of the spin fluctuation around a zone boundary, $Q = (\pi/a, \pi/a)$, Γ_Q , is markedly larger for both Tl2223 and Hg1223 than for YBCO_7 without a marked variation of the magnetic correlation length ξ_m . Since the spin-fluctuation-induced superconducting mechanism^{18,19} predicts a higher T_c for a larger $\Gamma_Q \xi_m^2$, the higher T_c in Tl2223 ($T_c = 115$ K) and Hg1223 ($T_c = 133$ K) than in YBCO_7 ($T_c = 93$ K) has been suggested to be due to an enhancement of $\chi_Q \Gamma_Q$.

As for the superconducting properties, the NMR results in Zn-doped YBCO_7 ,²⁰ Hg1223,²¹ Tl2223,²² Tl2201,²³ Bi2212,²⁴ and LSCO (Ref. 25) ($x \geq 0.20$) were consistently interpreted by the d -wave model in which the impurity scattering was incorporated in terms of the unitarity limit. With increasing experimental evidence that the order parameter (OP) is of the d -wave type with $d_{x^2-y^2}$ symmetry, the spin-fluctuation-mediated mechanism predicting the d wave for the high-temperature superconductivity becomes promising together with the intimate relationship between T_c and the AF spin correlation.

In order to obtain further firm evidence for the pairing mechanism of high- T_c superconductivity, we need more perspective information covering not only from the underdoped region near the insulator to superconducting boundary, but also the overdoped region involving the superconducting to metal boundary. So far, there have been few systematic experiments on the overdoped systems except for the Tl2201 compounds with a single CuO_2 layer. The $\text{TlSr}_2\text{CaCu}_2\text{O}_{7-\delta}$ (Tl1212) compound consists of the pyramidal CuO_2 bilayer in the unit cell,²⁶ as in YBCO_{6+x} , but without the CuO chain. T_c of these compounds is controlled by reducing oxygen in the TlO_2 layers and decreases monotonically from 70 K to 0 K with increasing oxygen content,²⁶ assuring that Tl1212 is in the overdoped regime as in Tl2201.¹⁰ The Hall coefficient R_H and the resistivity ρ exhibited the anomalous T dependences in the normal state,²⁶ as seen in other high- T_c materials. The former shows a broad peak for all compounds around 100–140 K, above which the Hall number $n_H = 1/R_H e$ exhibits a T -linear dependence. The latter, on the other hand, shows the power-law T dependence of $\rho = \rho_0 + T^n$ and the exponent n gradually changes from 1 to 2 with decreasing T_c , i.e., with increasing holes.

In this paper, we report extensive ^{63}Cu NMR investigations of the magnetic and the superconducting properties in a series of the overdoped Tl1212 compounds with $T_c = 70$ K, 52 K, and 10 K in order to elucidate the origin of the reduction in T_c with increasing holes and to unravel the symmetry of the OP of the superconductivity.

II. EXPERIMENTAL PROCEDURES

Tl1212 polycrystalline samples were prepared by the conventional solid-state reaction method described elsewhere.²⁶ T_c defined as the temperature below which the diamagnetic signal appears in ac susceptibility depends on the annealing condition. Three samples with $T_c = 70$ K, 52 K, and 10 K were confirmed to be of almost single phase by powder x-ray

diffraction experiments.²⁶ The sample was pulverized into grains with a size smaller than 20 μm in diameter for the NMR measurements. All grains were aligned along the c axis by use of the anisotropy of the susceptibility and fixed with a polymer in a magnetic field of ~ 11 T.

The NMR measurements were carried out by a conventional phase-coherent laboratory-built pulsed spectrometer by use of a superconducting magnet (12 T at 4.2 K). The ^{63}Cu NMR spectrum was obtained by using a boxcar integrator with sweeping magnetic field. The Knight shift, $1/T_1$, and $1/T_{2G}$ of ^{63}Cu were measured at $f = 125.1$ MHz over a T range of 1.4–250 K in ~ 11 T parallel and perpendicular to the c axis. $1/T_1$ was measured by the saturation recovery method. The nuclear relaxation function $R(t)$ for the central transition ($1/2 \leftrightarrow -1/2$) for $I = 3/2$ among the quadrupole split lines is given by²⁷

$$R(t) = \frac{M(\infty) - M(t)}{M(\infty)} = 0.9 \exp\left(-\frac{6t}{T_1}\right) + 0.1 \exp\left(-\frac{t}{T_1}\right), \quad (1)$$

where $M(t)$ is the nuclear magnetization at the time t after the saturation pulses. The spin-echo amplitude E , recorded as a function of time τ between the first and the second pulses, was fitted well to the expression²⁸

$$E(2\tau) = E_0 \exp\left[-\left(\frac{2\tau}{T_{2L}}\right) - \frac{1}{2} \left(\frac{2\tau}{T_{2G}}\right)^2\right], \quad (2)$$

where $1/T_{2G}$ is the Gaussian spin-echo decay rate associated with the indirect nuclear spin-spin coupling through the electronic excitations, and $1/T_{2L}$ is the Lorentzian decay rate associated with the nuclear spin-lattice relaxation process. $1/T_{2L}$ was determined from the expression of $1/T_{2L} = 3(1/T_1)_{\parallel} + (1/T_1)_{\perp}$.²⁹

III. EXPERIMENTAL RESULTS

A. ^{63}Cu NMR spectra and $^{63}\nu_Q$

Figures 1(a) and 1(b) show the ^{63}Cu NMR spectra at $T = 4.2$ K and $f = 125.1$ MHz for the compound with $T_c = 52$ K for the central transition ($1/2 \leftrightarrow -1/2$) in partially oriented powder with the c axis parallel and perpendicular to the external magnetic field, $H \sim 11$ T, respectively. As seen in each figure, a broad spectrum in the higher-field region arises from unoriented grains. Solid and dashed arrows correspond to respective peaks arising from grains with $\theta = 90^\circ$ and 41.8° to the c axis. From the integrated intensity ratio of the spectrum with the intense peak in the low-field region to that with the broad spectrum in the high-field region, the fraction of oriented grains with the c axis parallel to the field is anticipated to be $\sim 60\%$ of the whole sample. Since $1/T_1$ at the peak was uniquely determined with a single component in the normal state as described later, some contribution from the spectrum associated with unoriented grains was considered to be negligible, if any. The shift was precisely determined from the peak of the spectrum of oriented grains.

The full width at half maximum (FWHM) of the spectrum for $c \parallel H$ is about 300 Oe in the normal state, which is similar to those in other Bi- (Ref. 24) and Tl-based compounds,^{11,16} but is broader than for Y- and Hg-based compounds

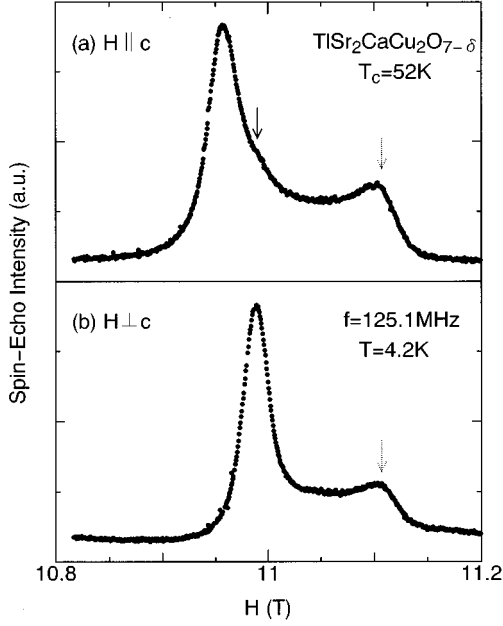


FIG. 1. ^{63}Cu NMR spectra of Tl1212 with $T_c = 52$ K at $T = 4.2$ K and $f = 125.1$ MHz for (a) $H \parallel c$ and (b) $H \perp c$. Solid and dashed arrows correspond to respective peaks arising from unoriented grains with $\theta = 90^\circ$ and 41.8° , where θ is the angle between the magnetic field and the c axis.

(≤ 100 Oe), suggesting that the homogeneity in the CuO_2 plane is somewhat worse than in Y- and Hg-based systems. In the case that H is perpendicular to the c axis, the shift consists of the Knight shift and the second-order quadrupole shift. The Knight shift perpendicular to the c axis, K_\perp , and the nuclear quadrupole frequency ν_Q can be expressed for the central transition ($1/2 \leftrightarrow -1/2$) of $I = 3/2$ according to second-order perturbation theory as follows:^{30,31}

$$\frac{\omega - ^{63}\gamma_N H_{\text{res}}}{^{63}\gamma_N H_{\text{res}}} = ^{63}K_\perp + \frac{3 \cdot ^{63}\nu_Q^2}{16(1 + ^{63}K_\perp)(^{63}\gamma_N H_{\text{res}})^2}, \quad (3)$$

where H_{res} is the resonance field, $^{63}\gamma_N$ the nuclear gyromagnetic ratio, and ω the NMR frequency, respectively. In order to separate the Knight shift from the quadrupole shift, the frequency (magnetic field) dependence of the spectrum has been measured at several different frequencies in a range of 80.1–125.1 MHz as seen in Fig. 2. From the slope of $(\omega - ^{63}\gamma_N H_{\text{res}})/^{63}\gamma_N H_{\text{res}}$ vs $(^{63}\gamma_N H_{\text{res}})^{-2}$ plots obtained from the ω dependence of H_{res} , $^{63}\nu_Q$'s are estimated to be ~ 20.7 , 22.5 , and 25.8 MHz for the Tl1212 compounds with $T_c = 70$ K, 52 K, and 10 K, respectively. Apparently, $^{63}\nu_Q$ increases with decreasing T_c , i.e., by doping holes.

B. Normal state

1. Knight shift

The bulk susceptibility in Tl1212, $\chi(T)$, revealed a small Curie-like upturn at low temperatures,²⁶ associated with the presence of Cu^{2+} impurities. So it is difficult to extract the intrinsic magnetic behavior from $\chi(T)$. By contrast, the local susceptibility at each atomic site can be obtained from the Knight shift without an influence of impurity spins. The

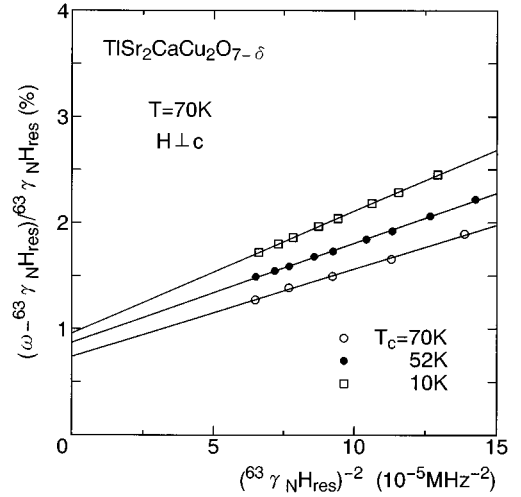


FIG. 2. $(\omega - ^{63}\gamma_N H_{\text{res}})/(^{63}\gamma_N H_{\text{res}})$ vs $(^{63}\gamma_N H_{\text{res}})^{-2}$ plots for Tl1212 with $T_c = 70$ K (\circ), 52 K (\bullet), and 10 K (\square). H_{res} 's are the resonance magnetic field for $H \perp c$ axis at various NMR frequencies in a range of 80.1–125.1 MHz.

Knight shift $K(T)$ in high- T_c cuprates consists of the T -independent orbital part K_{orb} and the T -dependent spin part $K_s(T)$,

$$K_\alpha(T) = K_{\text{orb},\alpha} + K_{s,\alpha}(T) \quad (\alpha = \perp, \parallel). \quad (4)$$

According to the Mila-Rice Hamiltonian,³² the spin Knight shift of ^{63}Cu in the CuO_2 plane, $^{63}K_s$, is expressed as

$$^{63}K_{s,\alpha}(T) = (A_\alpha + 4B)\chi_s(T) \quad (\alpha = \perp, \parallel), \quad (5)$$

where A_α and B are the on-site and the supertransferred hyperfine fields of ^{63}Cu , respectively, and $\chi_s(T)$ is assumed to be isotropic. A_α contains anisotropic dipole, spin-orbit, and isotropic core polarization contributions for the $\text{Cu } 3d_{x^2-y^2}$ orbit, and B originates from the isotropic $4s$ Fermi-contact type of the spin polarization produced by neighboring four Cu spins through the $\text{Cu}(3d_{x^2-y^2})\text{-O}(2p\sigma)\text{-Cu}(4s)$ hybridization.

Figures 3(a) and 3(b) show the T dependences of $^{63}K_\perp$ and $^{63}K_\parallel$ for the compounds with $T_c = 70$ K (\circ), 52 K (\bullet), and 10 K (\square), respectively. Both $^{63}K_\perp$ and $^{63}K_\parallel$ decrease rapidly below T_c for the compounds with $T_c = 70$ K (\circ) and 52 K (\bullet), demonstrating the spin-singlet-pairing state. In contrast to the underdoped systems in which $^{63}K_\parallel$ is dominated by the T -independent orbital contribution, $^{63}K_\parallel$ in Tl1212 exhibits a significant T dependence, reflecting the spin Knight shift. Furthermore, we note that T_c drops to ~ 63 K and 42 K for Tl1212 with $T_c = 70$ K and 52 K, respectively, by applying the magnetic field of ~ 11 T parallel to the c axis, similar to the case in Tl2201.^{11,23} In the normal state, it is remarkable that both shifts are T independent, pointing to the invariance of χ_s as in the case of YBCO₇ (Ref. 20) and Tl2201.^{11,23} Thus, the T -invariant χ_s is a common feature for the optimum-doped and the over-doped high- T_c cuprates in contrast to the decrease of $^{63}K_\perp$ upon cooling in underdoped LSCO,²⁵ Y124,³³ oxygen-deficient YBCO_{6+x},³⁴ and underdoped TlSr₂(Lu_{0.7}Ca_{0.3})Cu₂O_y ($T_c = 40$ K).⁸ Both shifts for the

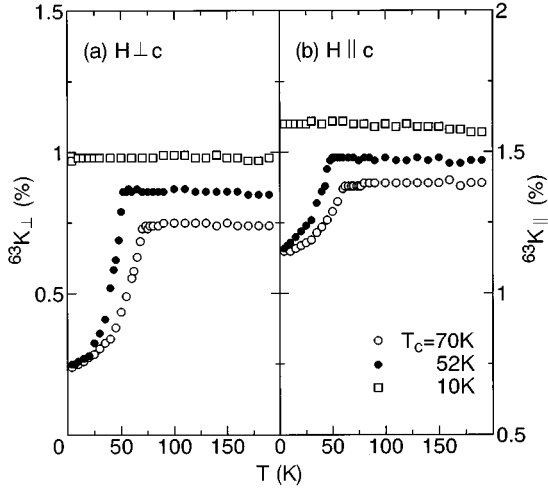


FIG. 3. T dependences of the Knight shifts (a) perpendicular, ${}^{63}K_{\perp}$, and (b) parallel, ${}^{63}K_{\parallel}$, to the c axis. \circ : $T_c = 70$ K. \bullet : 52 K. \square : 10 K.

compound with $T_c = 10$ K do not, however, exhibit an appreciable decrease, suggesting that the onset of the superconductivity is not well evidenced from the Knight shift measurements.

As seen in the figures, the respective residual Knight shifts at 4.2 K, $K_{\text{res},\perp}$ and $K_{\text{res},\parallel}$, are estimated to be 0.25% (0.26%) and 1.15% (1.16%) for the compound with $T_c = 70$ K (52 K). $K_{\text{res},\perp}$ and $K_{\text{res},\parallel}$ consist of the T -independent orbital and the residual spin shifts associated with the impurity scattering as argued extensively in the literatures.^{20–25} From the analysis of $1/T_1$ below T_c presented later, the residual fraction of the density of states (DOS) at the Fermi level, N_{res} , which contributes to the residual spin Knight shifts $K_{\text{res},s}$, is estimated to be $N_{\text{res}}/N_0 \sim 0.1$ where N_0 is defined as an effective DOS at T_c . Accordingly, by taking into account the residual fraction for both the spin shifts with $K_{\text{res},s}/K_s \sim 0.1$, $K_{\text{orb},\perp}$ and $K_{\text{orb},\parallel}$ are estimated to be 0.20% and 1.13%, respectively, for both compounds. For an estimation of ${}^{63}K_s$, ${}^{63}K_{\text{orb}}$ thus obtained is subtracted from the raw data above T_c . From Eq. (5), the anisotropy of ${}^{63}K_s$ is given by

$$\frac{{}^{63}K_{s,\parallel}}{{}^{63}K_{s,\perp}} = \frac{A_{\parallel} + 4B}{A_{\perp} + 4B}. \quad (6)$$

The anisotropy of ${}^{63}K_s$ in Tl1212 is evaluated as ~ 0.45 , 0.50, and 0.60 for the compounds with $T_c = 70$ K, 52 K, and 10 K, respectively. If the on-site hyperfine fields are assumed to be almost the same as those estimated in most of the high- T_c cuprates, being $A_{\perp} \sim 37$ kOe/ μ_B and $A_{\parallel} \sim -170$ kOe/ μ_B ,^{35–37} B 's are estimated to ~ 85 , 95, and 120 kOe/ μ_B from Eq. (6) for the compounds with $T_c = 70$ K, 52 K, and 10 K, respectively. As in the overdoped Tl2201,^{11,23} B in Tl1212 compounds increases with increasing oxygen content, being considerably larger than the typical value ($B \sim 40$ kOe/ μ_B) in underdoped LSCO,²⁵ Y124,³³ and YBCO_{6+x}.³⁴ Thus, it is deduced that the Cu($3d_{x^2-y^2}$)-O($2p\sigma$)-Cu($4s$) hybridization in the overdoped compounds is stronger than that in underdoped ones.

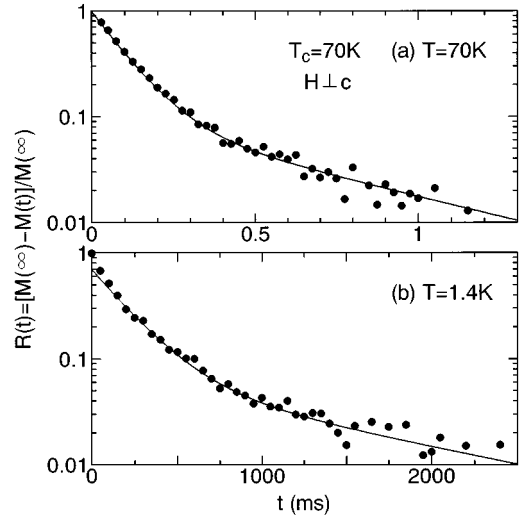


FIG. 4. Relaxation function, $R(t) = [M(\infty) - M(t)]/M(\infty)$, of the nuclear magnetization for the c axis $\perp H \sim 11$ T at (a) $T = 70$ K and (b) $T = 1.4$ K for the compound with $T_c = 70$ K. Here, $M(t)$ is the nuclear magnetization after the saturation pulses. Solid lines are best fits by the relaxation function of Eq. (1).

2. Nuclear spin-lattice relaxation rate $1/T_1$

Figures 4(a) and 4(b) show the relaxation curves of ${}^{63}\text{Cu}$, $R(t) = [M(\infty) - M(t)]/M(\infty)$, at $T = 70$ K above T_c and $T = 1.4$ K below T_c , respectively, for the compound with $T_c = 70$ K under the magnetic field of ~ 11 T perpendicular to the c axis. The solid curve is the best fit to Eq. (1). Although the orientation of the sample is not perfect, $R(t)$ above T_c was well fitted by Eq. (1) with a single T_1 component as seen in Fig. 4(a), assuring that the influence from unoriented grains is negligible.

Figure 5 shows the T dependence of ${}^{63}(1/T_1 T)_{\perp}$ for the compounds with $T_c = 70$ K (\circ), 52 K (\bullet), and 10 K (\square), respectively. In contrast to the T -invariant Knight shift, ${}^{63}(1/T_1 T)_{\perp}$ has a broad peak around $T^* \sim 90$ K, 70 K, and 30 K just above T_c for the compounds with $T_c = 70$ K, 52 K,

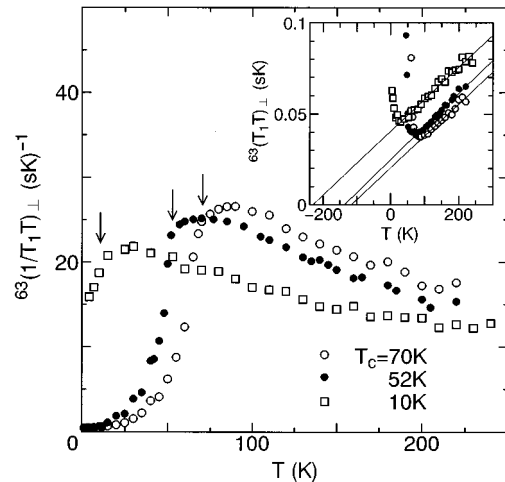


FIG. 5. T dependences of ${}^{63}(1/T_1 T)_{\perp}$. \circ : $T_c = 70$ K. \bullet : 52 K. \square : 10 K. Inset indicates the T dependence of ${}^{63}(T_1 T)_{\perp}$, proving that ${}^{63}(1/T_1 T)_{\perp}$ follows the Curie-Weiss behavior.

and 10 K, respectively. The T dependence of ${}^{63}(1/T_1T)_{\parallel}$ was confirmed to be quite similar to those of ${}^{63}(1/T_1T)_{\perp}$. In the inset of Fig. 5, ${}^{63}(1/T_1T)_{\perp}$ plotted against T reveals a T -linear dependence down to T^* , pointing to the Curie-Weiss behavior, $C/(T+\theta)$, of ${}^{63}(1/T_1T)_{\perp}$ down to T^* as observed for LSCO (Refs. 2,25) and YBCO₇,¹³ etc.

According to the Mila-Rice hyperfine Hamiltonian,³² ${}^{63}(1/T_1T)$ is expressed by

$${}^{63}(1/T_1T)_{\parallel} = -\frac{{}^{63}\gamma_N^2 k_B}{2\mu_B^2} \sum_q F_{\perp}(q)^2 \frac{\chi''(q, \omega)}{\omega},$$

$${}^{63}(1/T_1T)_{\perp} = \frac{{}^{63}\gamma_N^2 k_B}{4\mu_B^2} \sum_q [F_{\perp}(q)^2 + F_{\parallel}(q)^2] \frac{\chi''(q, \omega)}{\omega}, \quad (7)$$

where $\chi(q, \omega)$ is the dynamical susceptibility. The hyperfine form factors $F_{\parallel}(q)$ and $F_{\perp}(q)$ are given by

$$F_{\parallel}(q) = A_{\parallel} + 2B[\cos(q_x a) + \cos(q_y a)],$$

$$F_{\perp}(q) = A_{\perp} + 2B[\cos(q_x a) + \cos(q_y a)], \quad (8)$$

where a is the distance between the nearest-neighbor Cu atoms. Provided that $\chi(q, \omega)$ is dominated by the AF spin fluctuation around $Q = (\pi/a, \pi/a)$, ${}^{63}(1/T_1T)$ is proportional to $\chi_Q(T)$ in a two-dimensional (2D) square lattice. Accordingly, it is extracted that $\chi_Q(T)$'s in Tl1212 compounds follow the Curie-Weiss law as well as in the underdoped compounds.^{2,25} Thus, the Curie-Weiss behavior is the most universal characteristic in the high- T_c cuprates regardless of doping level. It is noteworthy that the Weiss constant θ of $\chi_Q(T)$ increases with increasing hole content as seen in the inset of Fig. 5. Remarkably, it was reported that the superconductivity no longer took place in Tl2201 which exhibited the $T_1 T = \text{const}$ relation over a wide T region, which is indicative of the intimate relationship with the presence of the AF spin fluctuation.

In order to embody the relationship between T_c and the AF spin fluctuation, we present the systematic change of the spin fluctuation spectrum described in terms of the dynamical susceptibility around $Q = (\pi/a, \pi/a)$,^{12,13}

$$\chi(Q+q, \omega) = \frac{\chi_{Q+q}}{1 - i\omega/\Gamma_{Q+q}}, \quad (9)$$

with

$$\chi_{Q+q} = \chi_Q / (1 + q^2 \xi_m^2),$$

$$\Gamma_{Q+q} = \Gamma_Q (1 + q^2 \xi_m^2),$$

$$\chi_Q = \alpha \xi_m^2, \quad (10)$$

where the parameters χ_Q , Γ_Q , ξ_m , and α are the AF spin susceptibility, the characteristic energy of the AF spin fluctuation, the magnetic coherence length (in a unit of a), and a scale factor to relate χ_Q to ξ_m^2 , respectively. By assuming a Lorentzian form for the energy distribution, the imaginary part of $\chi(q, \omega)$ is expressed as

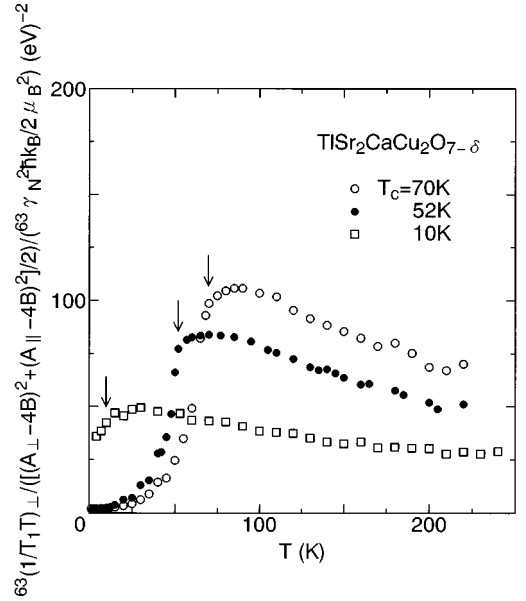


FIG. 6. T dependences of ${}^{63}(1/T_1T)_{\perp} / [(A_{\perp} - 4B)^2 + (A_{\parallel} - 4B)^2] / ({}^{63}\gamma_N^2 \hbar k_B / 2\mu_B^2)$ in Tl1212 with $T_c = 70$ K, 52 K, and 10 K, scaled approximately to $\sim \alpha/\hbar\Gamma_Q$.

$$\frac{\chi''(Q+q, \omega)}{\omega} = \frac{\chi_Q}{1 + q^2 \xi_m^2} \frac{\Gamma_{Q+q}}{\omega^2 + \Gamma_{Q+q}^2}; \quad (11)$$

for the system where the AF spin correlation prevails, i.e., $\xi_m \geq a$,

$${}^{63}(1/T_1T)_{\parallel} \approx \frac{{}^{63}\gamma_N^2 k_B}{2\mu_B^2} (A_{\perp} - 4B)^2 \frac{\chi_Q}{\Gamma_Q \xi_m^2},$$

$${}^{63}(1/T_1T)_{\perp} \approx \frac{{}^{63}\gamma_N^2 k_B}{4\mu_B^2} [(A_{\perp} - 4B)^2 + (A_{\parallel} - 4B)^2] \frac{\chi_Q}{\Gamma_Q \xi_m^2} \quad (12)$$

are derived since $\omega \rightarrow 0$ from Eq. (7). From Eq. (12), ${}^{63}(1/T_1T)$ is related to $\chi_Q/\Gamma_Q \xi_m^2 (= \alpha/\Gamma_Q)$. In order to extract the doping dependence of α/Γ_Q , ${}^{63}(1/T_1T)_{\perp}$ divided by the hyperfine form factor $[(A_{\perp} - 4B)^2 + (A_{\parallel} - 4B)^2]$ is presented in Fig. 6. In the overdoped Tl1212 compounds, Γ_Q in the compound with $T_c = 10$ K is larger than other higher T_c compounds and eventually its T dependence becomes weaker, suggesting that the AF spin fluctuation tends to be disrupted. In order to present the hole content dependence of α/Γ_Q with holes increasing from underdoped to overdoped compounds, the T dependence of ${}^{63}(1/T_1T)_{\parallel}$ divided by the hyperfine form factor $(A_{\perp} - 4B)^2$ for 10% and 15% Sr-doped LSCO,^{2,25} YBCO₇,²⁰ and Tl1212 with $T_c = 70$ K is shown in Fig. 7. It is evident that Γ_Q becomes larger with increasing hole content, which means that the spin fluctuation spectral weight is transferred to a higher-energy region as holes increase. Furthermore, from the anisotropy of the relaxation rate of ${}^{63}\text{Cu}$, ${}^{63}R = {}^{63}(1/T_1)_{\perp} / {}^{63}(1/T_1)_{\parallel}$, the q dependence of the spin fluctuation is extracted in an indirect manner. ${}^{63}R$ is evaluated using

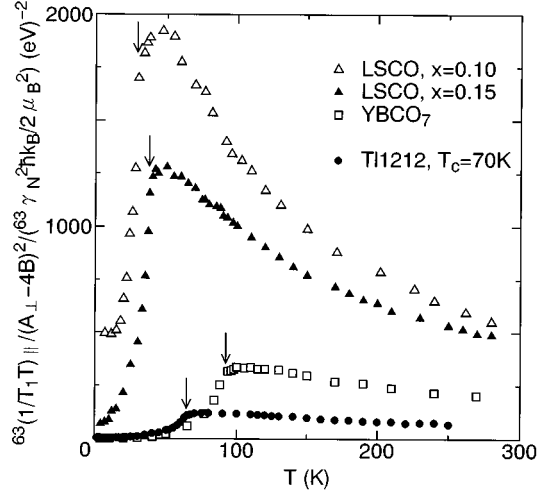


FIG. 7. T dependences of ${}^{63}(1/T_1 T)_\parallel / (A_\perp - 4B)^2 / ({}^{63}\gamma_N^2 \hbar k_B / 2\mu_B^2)$, scaled approximately to $\sim \alpha / \hbar \Gamma_Q$, for TI1212 with $T_c = 70$ K, YBCO₇,²⁰ 10% and 15% Sr-doped LSCO (Ref. 25).

the value of A_α and B in two limiting cases. In the case that $\chi(q)$ has a sharp peak at the zone boundary, ${}^{63}R_{AF}$ is obtained as

$${}^{63}R_{AF} = \frac{(A_\perp - 4B)^2 + (A_\parallel - 4B)^2}{2(A_\perp - 4B)^2}. \quad (13)$$

Provided that $\chi(q)$ is q independent, ${}^{63}R_r$ is obtained as

$${}^{63}R_r = \frac{(A_\perp^2 + 4B^2) + (A_\parallel^2 + 4B^2)}{2(A_\perp^2 + 4B^2)}. \quad (14)$$

${}^{63}R$ is nearly independent of the temperature and decreases with increasing holes as 1.7, 1.6, and 1.3 for the compounds with $T_c = 70$ K, 52 K, and 10 K, respectively. In Fig. 8, ${}^{63}R_{AF}$ and ${}^{63}R_r$ of the TI1212 compounds are plotted against

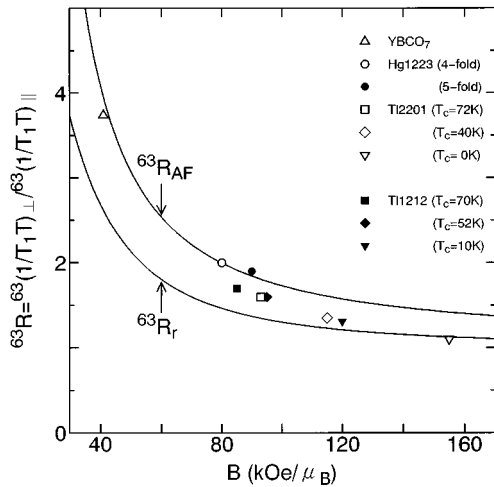


FIG. 8. ${}^{63}R$ [anisotropy of ${}^{63}(1/T_1 T)$] vs B (supertransferred hyperfine field) plots for various high- T_c cuprates (Ref. 11,17,38) with the hole content as an implicit parameter. ${}^{63}R_{AF}$ and ${}^{63}R_r$ are respective anisotropies for the case where the AF spin fluctuation prevails and is absent.

B with Eqs. (13) and (14), together with the results of Hg1223,¹⁷ YBCO₇,³⁸ and TI2201.¹¹ Here, $A_\perp = 37$ kOe/ μ_B and $A_\parallel = -170$ kOe/ μ_B are used for all compounds. As seen in the figure, ${}^{63}R$ in TI1212 is smaller than those in YBCO₇ and Hg1223, being close to ${}^{63}R_{AF}$, suggesting that the q dependence of the AF spin correlation around $Q = (\pi/a, \pi/a)$ is broad in TI1212. ${}^{63}R$ decreases progressively from ${}^{63}R_{AF}$ to ${}^{63}R_r$ with increasing B or holes. It is noteworthy that the AF spin correlations in TI1212 with $T_c = 10$ K and TI2201 with $T_c = 0$ K, both close to ${}^{63}R_r$, are considerably weakened and absent, respectively, showing that the presence of the AF spin fluctuation is responsible for the occurrence of superconductivity. We note that the spin fluctuation spectrum in q space as Γ_Q is shifted to a higher-energy region with the hole content. In order to shed further light on the novel nature of the spin correlation from another context, we next concern ourselves with $1/T_{2G}$ which enables us to measure ξ_m in a more direct manner.

3. Gaussian spin-echo decay rate, $1/T_{2G}$

As demonstrated by Pennington *et al.*,²⁸ since $1/T_{2G}$, which is dominated by the indirect nuclear spin-spin coupling through the electronic excitations in high- T_c cuprates, provides an important information on the real part of the q -dependent susceptibility $\chi(q)$. $1/T_{2G}$ is generally derived as^{39,40}

$$\left(\frac{1}{T_{2G}}\right)^2 = \frac{0.69({}^{63}\gamma_N \hbar)^4}{8\mu_B^4 \hbar^2} \left[\sum_q F_\parallel(q)^4 \chi(q)^2 - \left(\sum_q F_\parallel(q)^2 \chi(q) \right)^2 \right]. \quad (15)$$

In the case that the spatial spin correlation around $Q = (\pi/a, \pi/a)$ is decayed following $\exp(-r_{ij}/\xi_m)$, $\chi(Q) = \alpha \xi_m^2$ is obtained. As a consequence, $1/T_{2G}$ is given for $\xi_m \gg a$ by⁴⁰

$$\frac{1}{T_{2G}} \approx \sqrt{\frac{0.69}{32\pi}} \frac{{}^{63}\gamma_N^2 \hbar}{\mu_B^2} (A_\parallel - 4B)^2 \frac{\chi_Q}{\xi_m} (\propto \alpha \xi_m). \quad (16)$$

Accordingly, $1/T_{2G}$ is related to $\xi_m(T)$ [$\propto \sqrt{\chi_Q(T)}$]. In Fig. 9, the Gaussian spin-echo decay curves of ${}^{63}\text{Cu}$ at $T = 90$ K and ~ 11 T parallel to the c axis are plotted against the time, 2τ , between the first pulse and spin-echo for the compounds with $T_c = 70$ K (\circ), 52 K (\bullet), and 10 K (\square), respectively. All decay curves are well fitted to Eq. (2), assuring the expected Gaussian decay. The T dependence of $1/T_{2G}$ is displayed in Fig. 10 for the compounds with $T_c = 70$ K (\circ), 52 K (\bullet), and 10 K (\square), together with the data of YBCO₇ (Ref. 41). A remarkable feature is that $1/T_{2G}$ in TI1212 increases with decreasing temperature followed by a peak just above T_c as in Hg1223.¹⁷ At nearly the same temperature, ${}^{63}(1/T_1 T)$ exhibits a broad peak as well. In underdoped YBCO_{6+x} (Ref. 39) and Y124,⁴² which exhibit spin gap behavior, it should, however, be noted that $1/T_{2G}$ tends to saturate below the temperature where ${}^{63}(1/T_1 T)$ has a shallow peak far above T_c . In order to extract the doping dependence of $\alpha \xi_m$, $1/T_{2G}$ divided by the hyperfine form factor $(A_\parallel - 4B)^2$ in Eq. (16) is plotted in Fig. 11 together with the

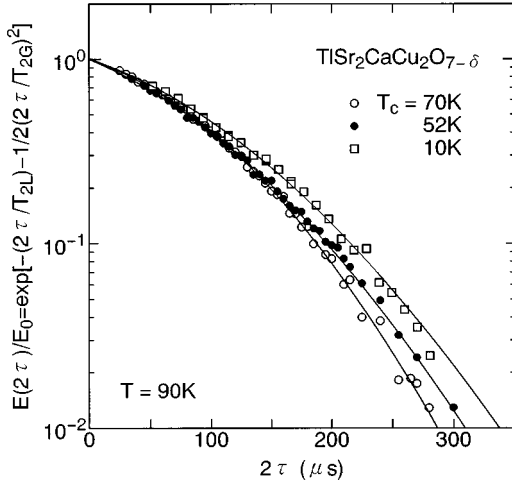


FIG. 9. Gaussian spin-echo decay curves at $T=90$ K. \circ : $T_c = 70$ K. \bullet : 52 K. \square : 10 K. τ is the time interval between the first and the second pulses. Solid lines are best fits by Eq. (2).

results of YBCO₇ (Ref. 41) and Hg1223.¹⁷ Interestingly, $\alpha\xi_m$ in Tl1212 is smaller than those in YBCO₇ and Hg1223, and is suppressed with increasing holes. As holes increase over an optimum doping, Γ_Q increases, whereas ξ_m is reduced. Eventually, T_c seems to be markedly suppressed. By contrast, provided that Γ_Q increases with ξ_m remaining nearly constant, T_c is significantly enhanced as demonstrated in the previous papers.^{16,17}

Moriya, Takahashi, and Ueda,¹² and Monthoux and Pines¹⁹ (MP) derived that T_c is proportional to $T_0 = \Gamma_Q \xi_m^2$ the effective bandwidth, i.e., the cutoff energy, based on the AF spin-fluctuation-mediated mechanism. In MP's expression, $T_c = \Gamma_Q \xi_m^2 [(1-\delta)/0.79] \exp(-1/\lambda) (\propto \chi_Q \Gamma_Q)$ was derived with $0.42 \leq \lambda \leq 0.48$ based on the strong-coupling calculation. These approaches have predicted that T_c is enhanced with increasing $\chi_Q \Gamma_Q$, which was confirmed experimentally.^{16,17} $\chi_Q \Gamma_Q$ is obtained from ${}^{63}(T_1 T)/(T_{2G})^2$ with the use of the following relation for $\xi_m \geq a$:⁴⁰

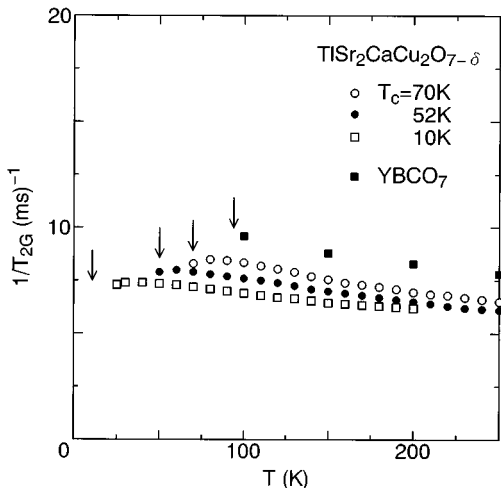


FIG. 10. T dependences of $1/T_{2G}$ in Tl1212 and YBCO₇ (Ref. 41). \circ : $T_c = 70$ K. \bullet : 52 K. \square : 10 K.

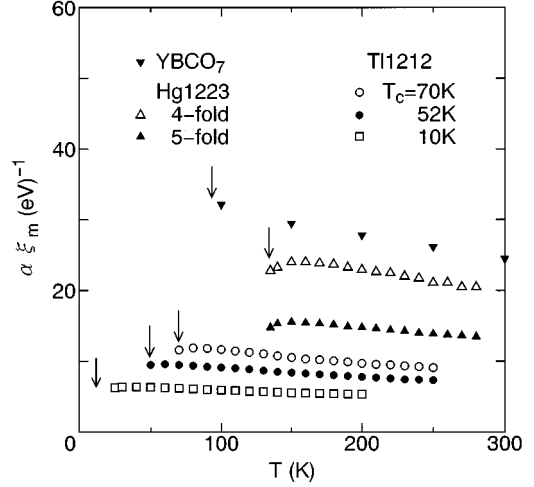


FIG. 11. T dependences of $\alpha\xi_m$ in Tl1212, together with the results for YBCO₇ (Ref. 41) and Hg1223 (Ref. 17).

$$\frac{{}^{63}(T_1 T)_{\parallel}}{(T_{2G})^2} \approx \frac{0.69({}^{63}\gamma_N \hbar)^2 F_{\parallel}(Q)^2}{16\pi\mu_B^2 \hbar k_B} (2 \times {}^{63}R - 1) (\chi_Q \hbar \Gamma_Q). \quad (17)$$

The magnitude of $\chi_Q \hbar \Gamma_Q$ is shown in the inset of Fig. 12 together with the results of YBCO₇ ($T_c = 93$ K) (Refs. 40,41) and Tl2201 ($T_c = 85$ K).⁴³ $\chi_Q \hbar \Gamma_Q$ is estimated to be ~ 1.4 , 1.2, and 1.0 for the compounds with $T_c = 70$ K, 52 K, and 10 K, respectively, being constant in a wide temperature range. This result is in contrast to the behavior of $T_1 T/T_{2G} (\propto \alpha \Gamma_Q \xi_m)$ being constant in the underdoped region.^{39,44,45} It is remarkable that the values of $\chi_Q \hbar \Gamma_Q$ in Tl1212's are smaller than that for YBCO₇ (~ 3.5) and Tl2201 (~ 1.9).

In order to uncover an intimate relationship between the magnetic excitation and the superconductivity in the optimum and the overdoped high- T_c cuprates, T_c 's are plotted against $\chi_Q \hbar \Gamma_Q$ and $\alpha\xi_m(T_c)$ for Hg1223,¹⁷ Tl2223,¹⁶ YBCO₇,⁴¹ Tl2201,⁴³ and Tl1212 in Figs. 13 and 14. In the

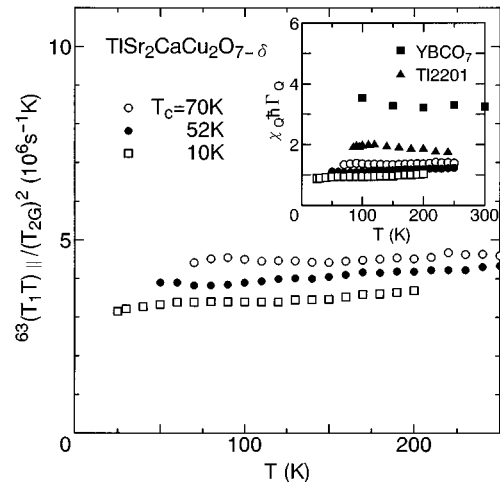


FIG. 12. T dependences of ${}^{63}(T_1 T)/(T_{2G})^2$ in Tl1212. \circ : $T_c = 70$ K. \bullet : 52 K. \square : 10 K. Inset is the comparison of the values of $\chi_Q \hbar \Gamma_Q$ with those for YBCO₇ (Ref. 41) and Tl2201 (Ref. 43).

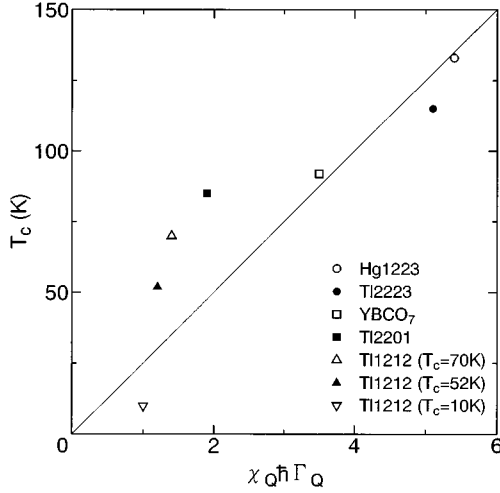


FIG. 13. T_c vs $\chi_Q \hbar \Gamma_Q$ plots for various high- T_c cuprates (Refs. 16,17,41,43).

figures, T_c 's in Hg1223, Tl2223, and YBCO₇ near an optimum hole doping increase linearly with an increase of $\chi_Q \hbar \Gamma_Q$, even though $\alpha \xi_m$ for the latter compounds with triple CuO₂ layers is smaller than for YBCO₇ with double layers. By contrast, nevertheless the reduction rate of $\chi_Q \hbar \Gamma_Q$ with the hole content in Tl1212 compounds is moderate, T_c drops rapidly as seen in Fig. 13. Apparently, T_c in Tl1212 is controlled by the different factors from $\chi_Q \hbar \Gamma_Q$. Namely, in the case of $\alpha \xi_m$ decreasing to less than a critical value of $\alpha \xi_m \sim 20$, the effective pairing interaction is weakened and hence λ is anticipated to be reduced.^{46–48}

C. Superconducting state

1. $1/T_1$

As presented in Sec. III B 2, the relaxation curve well below T_c is not fitted by Eq. (1) with a single T_1 component which is caused by the vortex cores. The short components arise from the nuclei close to the vortex cores, whereas the

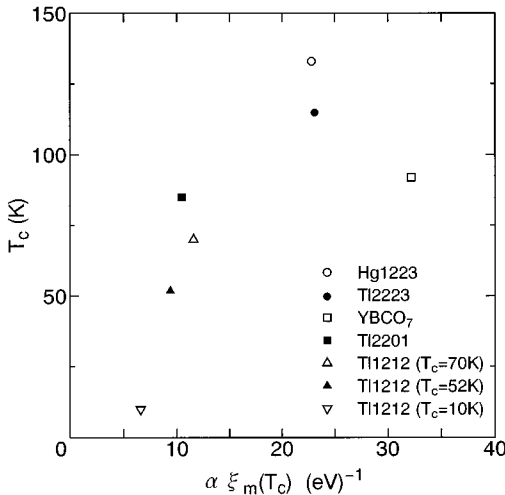


FIG. 14. T_c vs $\alpha \xi_m(T_c)$ plots for various high- T_c cuprates (Refs. 16,17,41,43).

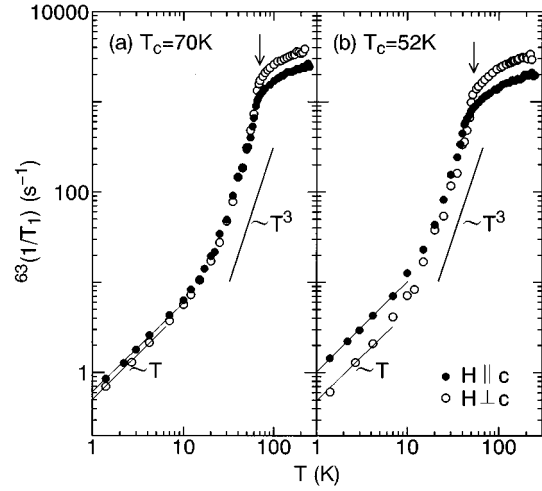


FIG. 15. T dependences of ${}^{63}(1/T_1)_\perp$ (○) and ${}^{63}(1/T_1)_\parallel$ (●) below T_c at ~ 11 T. (a) $T_c = 70$ K and (b) 52 K.

long components from those far away from the vortex cores. To display an overall T dependence of ${}^{63}(1/T_1)$ below T_c , the long component ${}^{63}(1/T_{1L})$ is tentatively extracted from a fit of Eq. (1) to $R(t)$ smaller than 0.5 as indicated by solid line in Fig. 4(b).

Figures 15(a) and 15(b) show the T dependence of ${}^{63}(1/T_{1L})_\perp$ (○) and ${}^{63}(1/T_{1L})_\parallel$ (●) below T_c plotted in logarithmic scales for the compounds with $T_c = 70$ K and 52 K, respectively. ${}^{63}(1/T_1)$'s for both samples decrease rapidly following a power-law-like T dependence below T_c without any enhancement just below T_c , which is the common behavior in most of high- T_c cuprates. At low temperatures well below T_c , it is evident that ${}^{63}(1/T_1)$ obeys the $T_1 T = \text{const}$ relation. In Fig. 16, $R(tT)$'s in a T range of 1.4–10 K well below T_c are plotted against the product of the time t and the temperature T , tT , for the compound with $T_c = 70$ K in ~ 11 T parallel to the c axis. $R(tT)$'s fall on a unique curve over a T range of 1.4–10 K, suggesting that all the ${}^{63}T_1$ components follow the $T_1 T = \text{const}$ relation at low temperatures regardless of the distribution of T_1 . The relaxation behavior in the superconducting mixed state is affected by fluxoid cores. An array of fluxoids gives rise to two different relaxation processes: (a) the thermal fluctuation of fluxoids which generates the transverse fluctuating field⁴⁹

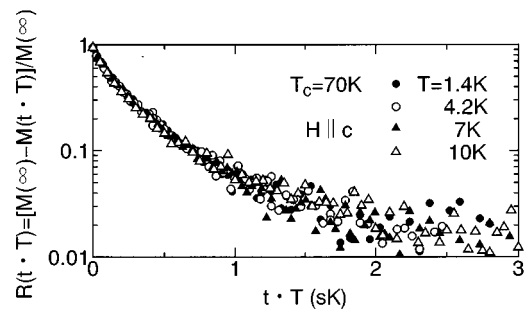


FIG. 16. Relaxation function, $R(tT)$, plotted against tT in a T range of 1.4–10 K for Tl1212 with $T_c = 70$ K. The result that $R(tT)$ is on a single curve probes that all the ${}^{63}T_1$ components follow the $T_1 T = \text{constant}$ law below 10 K.

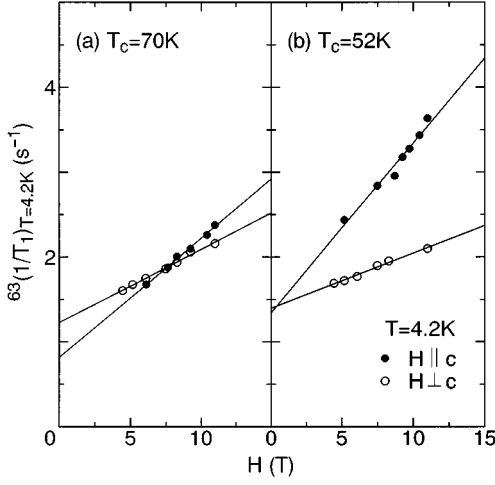


FIG. 17. Magnetic field dependences of ${}^{63}(1/T_1)$ parallel (●) and perpendicular (○) to the c axis at $T=4.2$ K. (a) $T_c=70$ K. (b) $T_c=52$ K.

and (b) the spin diffusion to vortex cores.⁵⁰ In the former, $1/T_1$ should be suppressed with increasing field, whereas in the latter, $1/T_1$ is enhanced with increasing the number of fluxoids. The nuclear relaxation measurements below T_c in the magnetic field were reported in YBCO₇,^{51,52} Y124,⁵³ and Hg1223,²¹ so far. From the result that the value of $1/T_1 T = \text{const}$ is linearly enhanced by the magnetic field, the nuclear relaxation for these compounds was shown to be dominated by the spin diffusion process to the vortex cores. By contrast, ${}^{63}(1/T_1)$ for Bi2212 (Ref. 24) and Tl2223,²² which followed the $T_1 T = \text{const}$ law, did not reveal any appreciable field dependence down to low temperatures. The T -linear dependence of $1/T_1$ in these compounds was concluded to be dominated by the presence of the residual DOS, at the Fermi level, N_{res} , rather than the vortex cores. As discussed extensively in the literatures,^{54–58} the gapless superconductivity caused by some imperfections presenting in the crystals provided an important clue to address the pairing state for high- T_c cuprates to be the d wave where the non-magnetic potential scattering acts as a pair breaker.

In order to investigate the relaxation process below T_c in Tl1212, the H dependence of ${}^{63}(1/T_1)$ was measured in a field range of 4–11 T. The H dependences of ${}^{63}(1/T_1)$ parallel (●) and perpendicular (○) to the c axis at $T = 4.2$ K for the compounds with $T_c = 70$ K and 52 K, respectively, are displayed in Fig. 17. As seen in the figure, ${}^{63}(1/T_1)$'s at low temperatures exhibit nearly H -linear dependences for both compounds. Furthermore, the H dependence is more pronounced in $H \parallel c$ than in $H \perp c$. In a rapid spin diffusion limit, $1/T_1$ is given by⁵⁹

$$(1/T_1)_{\text{obs},i} = (1/T_{1n} - 1/T_{1s})_i \frac{H}{\Phi} \xi_j \xi_k + (1/T_{1s})_i \quad (18)$$

$(i, j, k = \perp, \perp, \parallel),$

where $1/T_{1n}$ and $1/T_{1s}$ are the relaxation rates in and out of vortex cores, Φ is the flux quantum, and ξ_i is the superconducting coherence length along the i direction, respectively. $1/T_1$ is enhanced by the external magnetic field, and depends

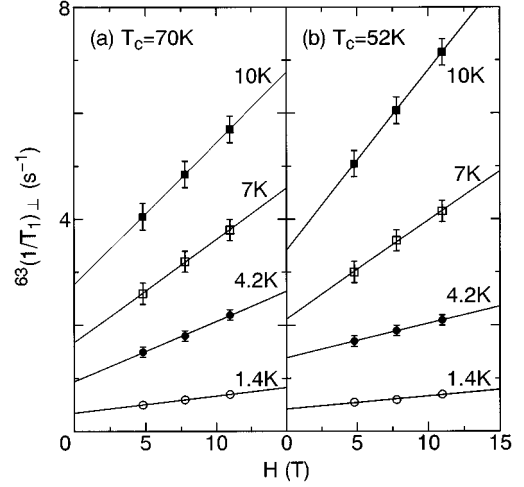


FIG. 18. Magnetic field dependences of ${}^{63}(1/T_1)_{\perp}$ in a T range of 1.4–10 K. (a) $T_c=70$ K and (b) $T_c=52$ K.

on the direction of the applied magnetic field due to the anisotropy of ξ_i ($\xi_{\perp} \geq \xi_{\parallel}$). Therefore, these experimental results prove that the relaxation process for Tl1212 is dominated by the spin diffusion process to the vortex cores at low temperatures as in the cases of YBCO₇,^{51,52} Y124,⁵³ and Hg1223,²¹ in contrast to the cases of Bi2212 (Ref. 24) and Tl2223.²² The fact that the $T_1 T = \text{const}$ relation holds at low temperatures under the magnetic field suggests that the electronic state in the vortex cores is described by the Fermi-liquid picture.^{52,53}

Figures 18(a) and 18(b) show the H dependences of ${}^{63}(1/T_1)_{\perp}$ for the compounds with $T_c = 70$ K and 52 K, respectively, in a T range of 1.4–10 K. ${}^{63}(1/T_{1s})_{\perp}$, inherent to the superconducting state, is determined from the extrapolation to zero field ($H \rightarrow 0$) according to Eq. (18). ${}^{63}(1/T_1)_{\text{obs}}$'s above 10 K were also confirmed to follow Eq. (18). The thus obtained T dependences for the compounds with $T_c = 70$ K and 52 K are presented in Figs. 19(a) and 19(b), respectively, where open (○) and solid (●) circles correspond to the raw $1/T_1$ data in ~ 11 T and ${}^{63}(1/T_{1s})_{\perp}$ estimated from the extrapolation to zero field in Fig. 18, respectively. It is remarkable that ${}^{63}(1/T_{1s})_{\perp}$ decreases over four orders of magnitude below T_c and behaves as ${}^{63}T_{1s} T = \text{const}$ below 10 K, indicative of the gapless nature of the superconductivity. Possible *in situ* imperfection, presumably existing associated with the oxygen content in Tl1212, may be responsible for the potential scattering, bringing about N_{res} as reported in many instances in the literatures.^{54–58} $1/T_1 T$ normalized at T_c , $(1/T_1 T)_{T_c}$, is related to the fraction of the residual DOS, N_{res}/N_0 , from a formula

$$\frac{(1/T_1 T)}{(1/T_1 T)_{T_c}} = \left(\frac{N_{\text{res}}}{N_0} \right)^2. \quad (19)$$

The fraction of N_{res}/N_0 is a measure to what extent the effective DOS is lost due to the onset of the superconductivity, and is estimated to be about ~ 0.10 for both samples with $T_c = 70$ K and 52 K from Eq. (19). The suppression in T_c by the nonmagnetic impurity in high- T_c cuprates was reported first by the NMR study on Zn-doped YBCO₇,²⁰ which was

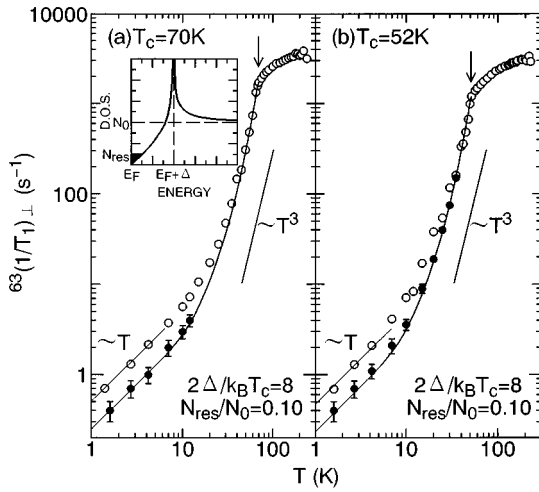


FIG. 19. T dependences of $^{63}(1/T_1)_\perp$ below T_c . (a) $T_c=70$ K. (b) $T_c=52$ K. Open (\circ) and solid (\bullet) circles indicate the raw data in ~ 11 T and $^{63}(1/T_{1s})_\perp$ extrapolated to zero magnetic field in Fig. 16, respectively. Solid lines are the calculation based on the gapless d -wave model with the parameters of $2\Delta/k_B T_c=8$ and $N_{\text{res}}/N_0=0.10$.

established by subsequent extensive experimental and theoretical works.^{54–58} The novel impurity and imperfection effects gave a decisive clue in identifying the OP of the high- T_c superconductivity to be of the d wave with $d_{x^2-y^2}$ symmetry together with the extensive theoretical works. A substantial aspect of the d -wave superconductivity with the line node is that even when T_c is moderately affected by impurities, the intrinsic gapless state with the line node changes into the gapless state with the finite DOS at the Fermi level. In general, it should be noted that T_c is controlled not only by the hole content, but also reduced by some imperfection and/or impurity. Since the amount of N_{res}/N_0 is nearly the same for two samples with $T_c=70$ K and 52 K, it is concluded that the reduction in T_c from 70 K to 52 K is not caused by a potential scattering, but by an increase of holes.

As indicated by solid lines in Figs. 19(a) and 19(b), the T dependences of $^{63}(1/T_{1s})_\perp$ in Tl1212 compounds are well interpreted by the gapless 2D d -wave model with $d_{x^2-y^2}$ symmetry where the energy gap vanishes along line at the cylindrical Fermi surface with the form of $\Delta(\phi) = \Delta_{\text{BCS}}(T) \cos(2\phi)$ together with N_{res} associated with the potential scattering as illustrated in the inset of Fig. 19. From the best fits to $^{63}(1/T_{1s})_\perp$ (\bullet), the parameters of $2\Delta/k_B T_c = 8$ and $N_{\text{res}}/N_0 = 0.10$ were deduced for both samples with $T_c = 70$ K and 52 K. Most remarkably, it is noteworthy that the same gapless d -wave-pairing model was consistently applied to the NMR results in Zn-doped YBCO₇,²⁰ Hg1223,²¹ Tl2223,²² Tl2201,²³ Bi2212,²⁴ and LSCO (Ref. 25) ($x \geq 0.20$) with nearly the same magnitude of the gap, $2\Delta/k_B T_c=8$, and the residual DOS fraction depending on the extent of the potential scattering in each compound. Without exception, the relaxation behavior in the superconducting state reported so far is in excellent agreement with the d -wave model. This conclusion is also supported by the Knight shift experiment as presented in the next section.

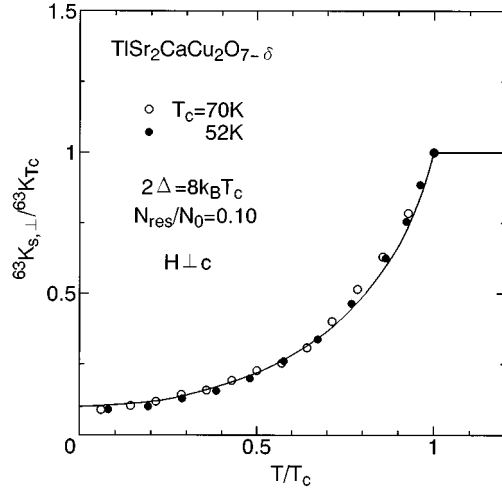


FIG. 20. T dependences of $^{63}K_{s,\perp}/^{63}K_{T_c}$ plotted against T/T_c . \circ : $T_c=70$ K. \bullet : 52 K. $^{63}K_{T_c}$ is the value of $^{63}K_{s,\perp}$ at T_c . Solid line is the calculation based on the gapless d -wave model with the same parameters as in the analyses of $^{63}(1/T_1)_\perp$ with $2\Delta/k_B T_c=8$ and $N_{\text{res}}/N_0=0.10$.

2. Knight shift

As displayed in Figs. 3(a) and 3(b), $^{63}K_\perp$ decreases below $T_c=70$ K and 52 K, whereas $^{63}K_\parallel$ decreases rapidly below $T_c \sim 63$ K and 42 K. T_c is more easily lowered by the magnetic field parallel than perpendicular to the c axis. N_{res} is induced not only by the potential scattering effects, but also by the magnetic field for the $H \parallel c$ axis. In order to avoid a complication to identify the origin of the residual DOS, we have analyzed the Knight shift data of ^{63}Cu for the $H \perp c$ axis in addition to $1/T_1$ where T_c is not significantly suppressed by the field. The residual shift at low temperatures is composed of the T -independent orbital shift and the residual spin shift originating from the finite DOS at the Fermi level. In order to estimate the T dependence of the spin Knight shift $^{63}K_{s,\perp}$, the orbital Knight shift $^{63}K_{\text{orb},\perp} = 0.20\%$ is subtracted from the raw data. The thus obtained T dependence of $^{63}K_{s,\perp}$ normalized by the value at T_c , $^{63}K_{s,\perp}/^{63}K_{T_c}$, is presented in Fig. 20, where the solid line is calculated using the gapless d -wave model with the same parameters of $2\Delta/k_B T_c=8$ and $N_{\text{res}}/N_0=0.10$ as those in the analyses of $^{63}(1/T_1)_\perp$ in the previous section. Thus, the results of both ^{63}K and $^{63}(1/T_1)_\perp$ are consistently understood in terms of the gapless d -wave model with the finite DOS at the Fermi level. From these experiments, it is concluded that superconductivity in the overdoped regime is of the d -wave type as confirmed in Tl2201.²³ Together with La- (Ref. 25) and Y-based systems,²⁰ the extensive NMR studies have clarified that the d -wave superconductivity is realized in high- T_c cuprates regardless of doping level.

IV. CONCLUSION

Whereas normal state properties in high- T_c cuprates are stressed to be quite anomalous in the underdoped region where spin gap behavior is of much interest, the present systematic NMR investigations in the overdoped Tl1212 have

unrevealed that the high- T_c cuprates share the common features regardless of doping level; that is, the AF spin fluctuation is present, yielding the Curie-Weiss law of $^{63}(1/T_1T)$ and the superconductivity is of the d -wave type.

Furthermore, the magnetic and the superconducting characteristics of the overdoped Tl1212 compounds were compared with the AF spin fluctuation model developed by Moriya, Takahashi, and Ueda, and Monthoux and Pines. Then, most of implications from such theories have been confirmed experimentally. Namely, the nuclear-spin lattice relaxation rate divided by temperature, $^{63}(1/T_1T) \propto \Gamma_Q^{-1}$, and the Gaussian spin-echo decay rate, $(1/T_{2G})^2 \propto \xi_m^2$, for ^{63}Cu have revealed the Curie-Weiss behavior for the compounds with $T_c = 70$ K, 52 K, and 10 K, leading to the relationship of $\Gamma_Q \xi_m^2 (\propto \chi_Q \Gamma_Q)$ being invariant with temperature. This experimental signature was predicted by the theories in which the dynamical susceptibility around $Q = (\pi/a, \pi/a)$, $\chi(Q, \omega)$, was described in terms of the Lorentzian forms with respect to both the wave number and the energy distribution.

As a natural consequence, above theories predicted the d -wave superconductivity mediated by the AF spin fluctuation and derived the novel relationship between T_c and the spin fluctuation parameters such as Γ_Q and ξ_m as follows:

$$T_c = \Gamma_Q \xi_m^2 [(1 - \delta)/0.79] \exp(-1/\lambda).$$

Actually, in the previous works, it was found from measurements of $1/T_1$ and $1/T_{2G}$ of ^{63}Cu that the significant enhancement of Γ_Q was the origin of the increase of T_c from 93 K in YBCO_7 to 115–133 K in Tl2223 and Hg1223 in the optimum-doped regime. Although ξ_m even decreases in Tl2223 and Hg1223, the increase of Γ_Q increases T_c linearly by the increase of the product of $\Gamma_Q \xi_m^2$, being in good agreement with the above formula.

By contrast, in the overdoped Tl1212 compounds, Γ_Q is transferred to a higher-energy region, while ξ_m concomitantly becomes smaller than those in the optimum-doped regime. Then, as holes increase, the AF spin correlation becomes less distinct. In spite of the rather slight decrease of $\Gamma_Q \xi_m^2$, the reduction rate in T_c for Tl1212 is much more pronounced than in the optimum-doped compounds (see Fig. 13). Eventually, the decrease of ξ_m , i.e., the suppression of the AF spin correlation, is anticipated to weaken the pairing interaction for the onset of the d -wave superconductivity, resulting in the decrease of λ in above formula.

λ seems to remain constant in the optimum doping region where ξ_m exceeds a critical value around $\alpha \xi_m \sim 20$. Therefore, the enhancement of Γ_Q makes T_c enhanced rather linearly. On the other hand, the increase of the hole content in going from the optimum-doped to the overdoped regime decreases ξ_m to less than the critical value under which λ starts to decrease appreciably. A change of the spin fluctuation spectrum with increasing hole content has been established from the present NMR experiments. In this context, the systematic NMR investigations from the optimum-doped to the overdoped high- T_c cuprates have allowed us to conclude that the spin-fluctuation-induced mechanism is most promising for the high- T_c superconductivity as long as the case is concerned with the optimum-doped and the overdoped regime.

ACKNOWLEDGMENTS

One of the authors (K.M.) would like to thank Dr. K. Ishida for valuable discussions. This work was partly supported by a Grant-in-Aid Scientific Research on Priority Areas ‘‘Science of High Temperature Superconductivity’’ from the Ministry of Education, Science of Culture.

¹For a review, see, for example, *Physica C* **235-240** (1994).

²Y. Kitaoka, S. Ohsugi, K. Ishida, and K. Asayama, *Physica C* **170**, 189 (1990); S. Ohsugi, Y. Kitaoka, K. Ishida, and K. Asayama, *J. Phys. Soc. Jpn.* **60**, 2351 (1991).

³W. W. Warren, Jr., R. E. Walstedt, G. F. Brennert, R. J. Cava, R. Tyckjo, R. F. Bell, and G. Dabbagh, *Phys. Rev. Lett.* **62**, 1193 (1989).

⁴H. Yasuoka, T. Imai, and T. Shimizu, *Strong Correlation and Superconductivity* (Springer-Verlag, Berlin, 1989) p. 254.

⁵H. Zimmermann, M. Mali, D. Brinkmann, J. Karpinsky, E. Kaldis, and S. Ruciecki, *Physica C* **159**, 681 (1989); T. Machi, T. Tomeno, T. Miyatake, N. Koshizuka, S. Tanaka, T. Imai, and H. Yasuoka, *Physica C* **173**, 32 (1990).

⁶J. Rossat-Mignod, L. P. Regnault, C. Vettier, P. Burllet, J. Y. Henry, and G. Lapertot, *Physica B* **169**, 58 (1991); J. Rossat-Mignod, L. P. Regnault, C. Vettier, P. Bourges, P. Burllet, J. Bossy, J. Y. Henry, and G. Lapertot, *Physica C* **185-189**, 89 (1991); J. Rossat-Mignod, L. P. Regnault, P. Bourges, C. Vettier, P. Burllet, and J. Y. Henry, *Physica B* **186-188**, 1 (1993).

⁷T. Tanamoto, K. Kohno, and H. Fukuyama, *J. Phys. Soc. Jpn.* **61**, 1886 (1992); **62**, 717 (1993); **62**, 1455 (1993); **63**, 2739 (1994).

⁸K. Magishi, Y. Kitaoka, G.-q. Zheng, K. Asayama, T. Kondo, Y.

Shimakawa, T. Manako, and Y. Kubo, *Phys. Rev. B* (to be published).

⁹T. Mito, Y. Kitaoka, T. Tanaka, K. Ishida, and K. Asayama (unpublished).

¹⁰Y. Shimakawa, Y. Kubo, T. Manako, and H. Igarashi, *Phys. Rev. B* **40**, 11 400 (1989); **42**, 10 165 (1990); Y. Kubo, Y. Shimakawa, T. Manako, and H. Igarashi, *ibid.* **43**, 7875 (1991).

¹¹Y. Kitaoka, K. Fujiwara, K. Ishida, K. Asayama, Y. Shimakawa, T. Manako, and Y. Kubo, *Physica C* **179**, 107 (1991).

¹²T. Moriya, Y. Takahashi, and K. Ueda, *J. Phys. Soc. Jpn.* **59**, 2905 (1990).

¹³A. J. Mills, H. Monien, and D. Pines, *Phys. Rev. B* **42**, 167 (1990).

¹⁴N. Bulut and D. J. Scalapino, *Phys. Rev. Lett.* **67**, 2898 (1991); *Phys. Rev. B* **45**, 2371 (1992).

¹⁵K. Levin, J. H. Kim, J. P. Lu, and Q. Si, *Physica C* **175**, 449 (1991); Y. Zha, Q. Si, and K. Levin, *ibid.* **212**, 413 (1993); Q. Si, Y. Zha, K. Levin, and J. P. Lu, *Phys. Rev. B* **47**, 9055 (1993).

¹⁶G.-q. Zheng, Y. Kitaoka, K. Asayama, K. Hamada, H. Yamauchi, and S. Tanaka, *J. Phys. Soc. Jpn.* **64**, 2524 (1995).

¹⁷K. Magishi, Y. Kitaoka, G.-q. Zheng, K. Asayama, K. Tokiwa, A.

- Iyo, and H. Ihara, *J. Phys. Soc. Jpn.* **64**, 4561 (1995).
- ¹⁸T. Moriya and K. Ueda, *J. Phys. Soc. Jpn.* **63**, 1871 (1994).
- ¹⁹P. Monthoux and D. Pines, *Phys. Rev. B* **47**, 6069 (1993); **49**, 4261 (1994).
- ²⁰K. Ishida, Y. Kitaoka, N. Ogata, T. Kamino, K. Asayama, J. R. Cooper, and N. Athanassopoulou, *J. Phys. Soc. Jpn.* **62**, 2803 (1993).
- ²¹K. Magishi, Y. Kitaoka, G.-q. Zheng, K. Asayama, K. Tokiwa, A. Iyo, and H. Ihara, *Phys. Rev. B* **53**, R8906 (1996).
- ²²G.-q. Zheng, Y. Kitaoka, K. Asayama, K. Hamada, H. Yamauchi, and S. Tanaka, *Physica C* **260**, 197 (1996).
- ²³K. Fujiwara, Y. Kitaoka, K. Ishida, K. Asayama, Y. Shimakawa, T. Manako, and Y. Kubo, *Physica C* **184**, 207 (1991).
- ²⁴K. Ishida, Y. Kitaoka, K. Asayama, K. Kadowaki, and T. Mochiku, *J. Phys. Soc. Jpn.* **63**, 1104 (1994).
- ²⁵S. Ohsugi, Y. Kitaoka, K. Ishida, G.-q. Zheng, and K. Asayama, *J. Phys. Soc. Jpn.* **63**, 700 (1994).
- ²⁶Y. Kubo, T. Kondo, Y. Shimakawa, T. Manako, and H. Igarashi, *Phys. Rev. B* **45**, 5553 (1992).
- ²⁷A. Narath, *Phys. Rev. B* **13**, 3724 (1976).
- ²⁸C. H. Pennington, D. J. Durand, C. P. Slichter, J. P. Rice, E. D. Bukowski, and D. M. Ginsberg, *Phys. Rev. B* **39**, 274 (1989); C. H. Pennington and C. P. Slichter, *Phys. Rev. Lett.* **66**, 381 (1991).
- ²⁹R. E. Walstedt and S-W. Cheong, *Phys. Rev. B* **51**, 3163 (1995).
- ³⁰A. Abragam, *The Principles of Nuclear Magnetism* (Clarendon, Oxford, 1961).
- ³¹M. Takigawa, P. C. Hammel, R. H. Heffner, Z. Fisk, J. L. Smith, and R. Schmary, *Phys. Rev. B* **39**, 300 (1989).
- ³²F. Mila and T. M. Rice, *Physica C* **157**, 561 (1989); *Phys. Rev. B* **40**, 11 382 (1989).
- ³³H. Zimmermann, M. Mali, M. Bamky, and D. Brinkmann, *Physica C* **185-189**, 9574 (1990).
- ³⁴M. Takigawa, A. D. Reyes, P. C. Hammel, J. D. Thompson, R. H. Heffner, Z. Fisk, and K. C. Ott, *Phys. Rev. B* **43**, 247 (1991).
- ³⁵H. Monien, D. Pines, and M. Takigawa, *Phys. Rev. B* **43**, 258 (1991).
- ³⁶H. Monien, P. Monthoux, and D. Pines, *Phys. Rev. B* **43**, 275 (1991).
- ³⁷T. Imai, *J. Phys. Soc. Jpn.* **59**, 2508 (1990).
- ³⁸S. E. Barrett, J. A. Martindale, D. J. Durand, C. H. Pennington, C. P. Slichter, T. A. Friedmann, J. P. Rice, and D. M. Ginsberg, *Phys. Rev. Lett.* **66**, 108 (1991).
- ³⁹M. Takigawa, *Phys. Rev. B* **49**, 4158 (1994).
- ⁴⁰D. Thelen and D. Pines, *Phys. Rev. B* **49**, 3528 (1994).
- ⁴¹T. Imai, C. P. Slichter, A. P. Paulikas, and B. Veal, *Phys. Rev. B* **47**, 9158 (1993).
- ⁴²Y. Itoh, H. Yasuoka, Y. Fujiwara, Y. Ueda, T. Machi, I. Tomeno, K. Tai, N. Koshizuka, and S. Tanaka, *J. Phys. Soc. Jpn.* **61**, 1287 (1992).
- ⁴³Y. Itoh, H. Yasuoka, A. Hayashi, and Y. Ueda, *J. Phys. Soc. Jpn.* **63**, 22 (1994).
- ⁴⁴R. L. Corey, N. J. Curro, K. O'Hara, T. Imai, C. P. Slichter, K. Yoshimura, M. Katoh, and K. Kosuge, *Phys. Rev. B* **53**, 5907 (1996).
- ⁴⁵T. Imai, C. P. Slichter, K. Yoshimura, M. Katoh, and K. Kosuge, *Phys. Rev. Lett.* **71**, 1254 (1993).
- ⁴⁶J. E. Hirsch and D. J. Scalapino, *Phys. Rev. Lett.* **56**, 2732 (1986).
- ⁴⁷P. Monthoux, A. V. Balatsky, and D. Pines, *Phys. Rev. Lett.* **67**, 3448 (1991); *Phys. Rev. B* **46**, 14 803 (1992).
- ⁴⁸P. Monthoux and D. Pines, *Phys. Rev. Lett.* **69**, 961 (1992).
- ⁴⁹E. Ehrenfreund, I. B. Goldberg, and M. Weger, *Solid State Commun.* **7**, 1333 (1969).
- ⁵⁰C. Caroli and J. Matricon, *Phys. Kondens. Mater.* **3**, 380 (1965).
- ⁵¹J. A. Martindale, S. E. Barrett, D. J. Durand, K. E. O'Hara, C. P. Slichter, W. C. Lee, and D. M. Ginsberg, *Phys. Rev. B* **50**, 13 645 (1994).
- ⁵²K. Ishida, Y. Kitaoka, and K. Asayama, *Solid State Commun.* **90**, 563 (1994).
- ⁵³G.-q. Zheng, Y. Kitaoka, K. Asayama, and Y. Kodama, *Physica C* **227**, 169 (1994).
- ⁵⁴S. Schmitt-Rink, K. Miyake, and C. M. Varma, *Phys. Rev. Lett.* **57**, 2575 (1986).
- ⁵⁵P. J. Hirschfeld, D. Vollhardt, and P. Wolfe, *Solid State Commun.* **59**, 111 (1986).
- ⁵⁶T. Hotta, *J. Phys. Soc. Jpn.* **62**, 7895 (1993).
- ⁵⁷P. J. Hirschfeld and N. Goldenfeld, *Phys. Rev. B* **48**, 4219 (1993).
- ⁵⁸S. Schmitt-Rink, K. Miyake, and C. M. Varma (unpublished).
- ⁵⁹I. B. Goldberg and M. Weger, *J. Phys. Soc. Jpn.* **24**, 1279 (1968).